

# Improving poor fill factors for solar cells via light-induced plating\*

Xing Zhao(邢钊)<sup>†</sup>, Jia Rui(贾锐)<sup>†</sup>, Ding Wuchang(丁武昌), Meng Yanlong(孟彦龙), Jin Zhi(金智), and Liu Xinyu(刘新宇)

Institute of Microelectronics, Chinese Academy of Sciences, Beijing 100029, China

**Abstract:** Silicon solar cells are prepared following the conventional fabrication processes, except for the metallization firing process. The cells are divided into two groups with higher and lower fill factors, respectively. After light-induced plating (LIP), the fill factors of the solar cells in both groups with different initial values reach the same level. Scanning electron microscope (SEM) images are taken under the bulk silver electrodes, which prove that the improvement for cells with a poor factor after LIP should benefit from sufficient exploitation of the high density silver crystals formed during the firing process. Moreover, the application of LIP to cells with poor electrode contact performance, such as nanowire cells and radial junction solar cells, is proposed.

**Key words:** solar cells; light-induced plating; fill factor; silver crystal

**DOI:** 10.1088/1674-4926/33/9/094008

**PACC:** 8630J

## 1. Introduction

In silicon solar cells, metallization of both surfaces is carefully optimized<sup>[1]</sup> to ensure a low series resistance and a high shunt resistance, which result in a high fill factor. However, the fill factor enhancement is restricted by high series resistances. The series resistance of a silicon solar cell is mainly composed of three parts<sup>[2]</sup>: sheet resistance of the emitter, conducting resistance of the grid lines on the front surface and contact resistance between the front electrode and the emitter. Among the three parts, the contact resistance may be the most significant, which should be carefully optimized for cell efficiency enhancement.

The contact performance usually depends on the firing process. After firing, three current paths between the bulk silver and the emitter are formed<sup>[3]</sup>, among which the contact of the bulk silver and the silver crystals embedded in the emitter results in the lowest contact resistance, as the resistance between the silver crystal and the emitter is extremely low. Huljic and Ballif<sup>[4]</sup> demonstrated that the typical contact resistance of a silver crystallite in contact to an n-emitter with a sheet resistance of  $R_{sh} = 30 \Omega/\square$  is between  $4 \times 10^{-8}$  and  $2 \times 10^{-7} \Omega \cdot \text{cm}^2$ , which is investigated by conductive atom force microscope (AFM) measurement.

The light-induced-plating (LIP) technique has drawn considerable attention as an effective method to optimize the cell front contact based on the two-layer model<sup>[5]</sup>. The two-layer model was initially proposed to make contact grids narrower and thicker. As is known, metallization of the front surface is generally fulfilled by using the screen printing method<sup>[6]</sup>. However, screen printing is not fully able to meet the requirements for narrower and thicker guidelines, as the paste flows aside during the annealing process, which limits the aspect ratio to a relatively low level. In the two layer model, a narrow and thin layer is firstly screen printed (or by aerosol jet printing<sup>[7]</sup>, etc.) and fired

as the seed layer, which is thickened by a subsequent light-induced plated layer. Besides the contact grid modifications, an unexpected phenomenon was observed that the contact resistance between the bulk silver and the emitter was reduced.

Research has shown that four new current paths are created after LIP<sup>[2]</sup>. The most important one is the direct contact of the plated silver with silver crystals. The contact resistance can be very low if the silver crystals are sufficiently created and contacted to bulk silver.

The front emitter needs a lightly doped profile to ensure a low saturation current. However, the contact resistance between the high sheet resistance emitter and the metallization is too high. Several techniques have been developed to solve this problem, such as LIP, the selective emitter (SE) solar cell concept<sup>[8]</sup>, and developing a new kind of silver paste<sup>[9]</sup>. In the SE concept, a heavily doped area is formed under the metallization, while the left of the emitter is still lightly doped. Paste development is also successful for the improvement of contact performance. However, the SE solar cell concept requires the formation of a selected heavily doped area, which adds to the total costs, as well as the alignment requirement, and so the self-aligned SE method<sup>[10]</sup> is not suitable for the present industrial metallization method (the screen printing method). Moreover, despite developments of the silver paste, it is still unsuitable for obtaining grid lines with high aspect ratios. LIP combined with the two-layer model successfully fulfills the above two functions<sup>[11]</sup>, which is the most advantageous of the three methods.

In order to investigate the potential application of LIP on silicon solar cells, experiments are carried out on silicon solar cells with poor fill factors limited by high series resistances. Cell performances before and after LIP are compared. Results show that LIP can effectively ameliorate the poor fill factors by reducing series resistances.

\* Project supported by the National Natural Science Foundation of China (Nos. 11104319, 51172268, 2009CB939703).

<sup>†</sup> Corresponding author. Email: qihuangshu@163.com, jiarui@ime.ac.cn

Received 21 February 2012, revised manuscript received 20 March 2012

© 2012 Chinese Institute of Electronics

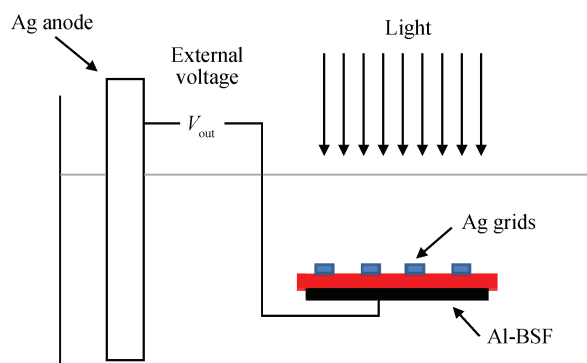


Fig. 1. Schematic diagram of light-induced plating (LIP).

## 2. Principle of light-induced plating

The schematic diagram is shown in Fig. 1. The metalized solar cell is located inside the  $\text{AgNO}_3$  electrolyte with its front surface exposed to light. An absorbed photon creates an electron-hole pair in the cell, and the pair is separated by the built-in electric field. Electrons go to Ag grids on the front surface and combine with  $\text{Ag}^+$ , resulting in the plating of Ag on the front Ag grids. Holes go to the back of the cell and cause the Al-BSF to dissolve. In order to protect the Al-BSF from being dissolved, an external voltage is applied between the Ag anode and the Al-BSF. The external voltage forces the Ag anode to lose electrons so that the Al-BSF keeps unchanged. We set up our own LIP equipment and achieved compact plated silver on a screen-printed Ag seed layer, as is shown in Fig. 4(a).

## 3. Effects of LIP on solar cells

### 3.1. Improvement in fill factor

Solar cells are fabricated on a batch of  $40 \times 40 \text{ mm}^2$  solar grade single-crystal wafers. All processes follow conventional techniques, except for the co-firing step, which is conducted in an annealing tube under  $\text{O}_2$  ambience with a gas flow of 1 L/min. After co-firing of the front and back contacts, the cells are rinsed in  $\text{AgNO}_3$  electrolyte for several minutes for light-induced plating.  $I$ - $V$  characteristics, as well as series resistances of the cells before and after LIP are tested for comparisons of cell performances. External quantum efficiency (EQE) and internal quantum efficiency (IQE) before and after LIP are also achieved.

Cell performances before and after light-induced plating are compared in Tables 1 and 2, where  $V_{oc}$  is the open circuit voltage,  $I_{sc}$  is the short circuit current density, FF is the fill factor,  $\eta$  is the efficiency, and  $R_s$  is the series resistance.

The low  $I_{sc}$  values for the processed cells are due to a terrible shading loss from having too-wide front side gridlines, as a problem occurs with our screen-printer. Another cause of the low  $I_{sc}$  may originate from the non-optimized annealing condition. However, we are more interested in their fill factors. The cells processed under the same temperature results in great difference in fill factors, as in the two groups A and B shown above. In group A, the cells exhibit low fill factors while the cells in group B exhibit relatively higher fill factors. After LIP for several minutes, fill factors in both groups reach the same

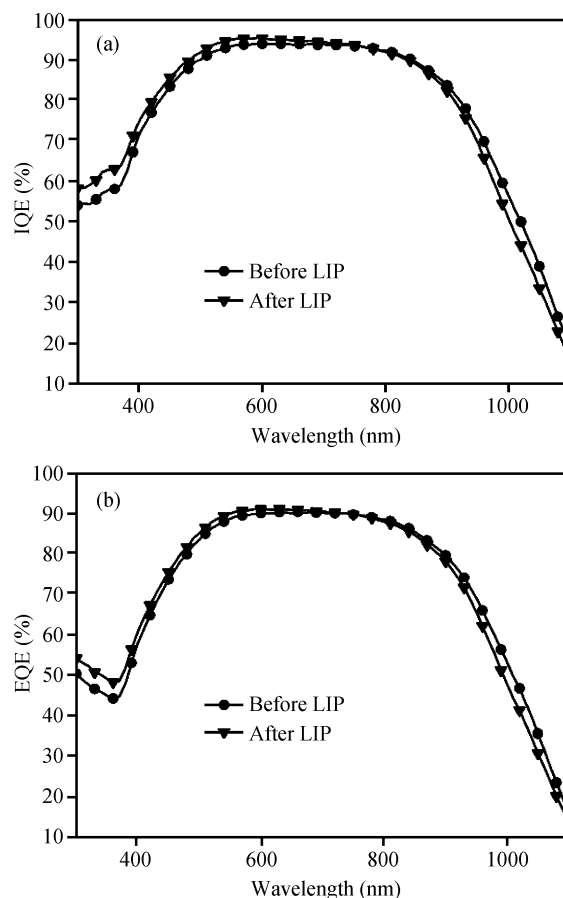


Fig. 2. (a) Comparison of IQE before and after LIP. (b) Comparison of EQE before and after LIP.

level. For group A, after LIP fill factor reaches 0.70. An enhancement of 31% compared with the fill factor before LIP is achieved. Meanwhile, the series resistance drops from 0.60 to 0.11  $\Omega$ . However, for group B, the fill factors almost remain unchanged after LIP, though their series resistance drops from 0.079 to 0.038  $\Omega$ .

The differences between the two groups may be explained as follows: silver crystals reach the same level after the firing process, which results in the similar fill factor potential for cells in group A and B. However, in group A, during the cooling down phase, the bulk silver shrinks and thus causes insufficient contact with silver crystals. Consequently, the contact resistance becomes very high and thus leads to a low fill factor. Electrolytes penetrate to the porous screen-printed silver and the plated silver contacts with the idle silver crystals during the LIP process. By using LIP, a low series resistance is achieved, which contributes prominently to the great improvement in the fill factor of the cell. For group B, low series resistance is already achieved and few crystals are idle. Contact resistance is now a secondary factor in series resistance and the reduction in conducting resistance by thickening the front grids becomes ignorable. As series resistance is already located at a low level, its reduction will contribute little to the improvement in fill factor.

Comparisons of external quantum efficiency (EQE) and internal quantum efficiency (IQE) before and after LIP are presented in Figs. 2(a) and 2(b).

Table 1. Group A, performances comparison for cells with low fill factor before and after LIP.

Process sequence	$V_{oc}$ (V)	$I_{sc}$ (mA/cm <sup>2</sup> )	FF (%)	$\eta$ (%)	$R_s$ ( $\Omega$ )
Before LIP	0.614	27.9	39.0	6.7	0.60
After LIP	0.616	27.1	70.0	11.7	0.11

Table 2. Group B, performances comparison for cells with high fill factor before and after LIP.

Process sequence	$V_{oc}$ (V)	$I_{sc}$ (mA/cm <sup>2</sup> )	FF (%)	$\eta$ (%)	$R_s$ ( $\Omega$ )
Before LIP	0.612	27.5	71.0	11.9	0.079
After LIP	0.613	26.8	72.5	11.9	0.038

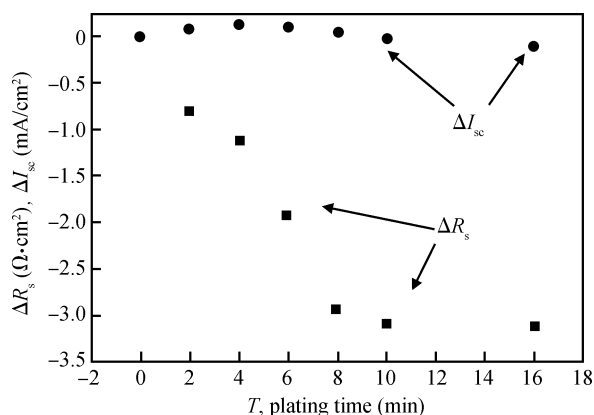


Fig. 3. Variation of  $R_s$  and  $I_{sc}$  with the plating time ( $\Delta R_s$ : Relative resistance increase;  $\Delta I_{sc}$ : Relative short circuit current density increase).

Figures 2(a) and 2(b) show that quantum efficiency (either IQE or EQE) slightly differs after and before LIP. After LIP, quantum efficiency (QE) rises in the short wavelength region ( $< 700$  nm) while it decreases in the long wavelength region ( $> 900$  nm).

The increase of QE in the short wavelength region may be attributed to the spreading of the plated silver into the interface between the bulk silver and the emitter. The decrease of QE in the long wavelength region may originate from the BSF (back surface field) peeling off slightly during the LIP process, which leads to extra light transmission.

### 3.2. Effects of the light-induced plating time on $R_s$ and $I_{sc}$

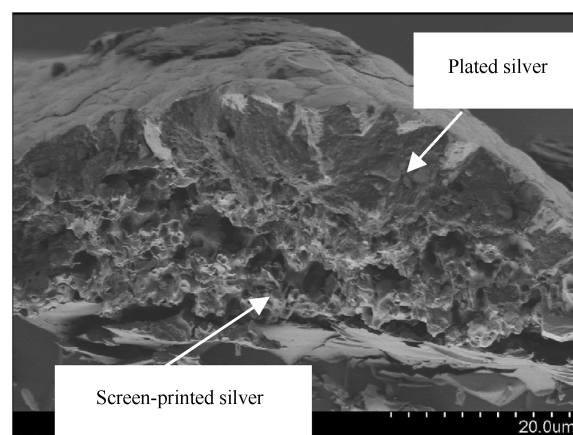
The variation of series resistance  $R_s$  and short circuit current density  $I_{sc}$  of the solar cell during the LIP process is shown in Fig. 3.

$R_s$  is significantly reduced during the first few minutes and then slide gently with the plating time. The significant reduced resistance can be explained as the reduction of contact resistance, while the slightly reduced resistance may be owed to the thickening of the grids.

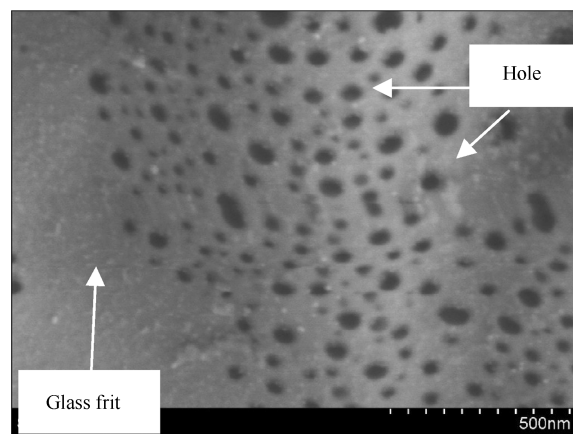
$I_{sc}$  slightly rises and then slightly decreases. The rise of  $I_{sc}$  is due to the increase of QE in short wavelength region, while the reduction due to the increasing shading loss of the broadening grids during LIP.

### 3.3. Comparison of LIP and electroplating

Electroplating has also proven its effectiveness in reduc-



(a)



(b)

Fig. 4. (a) SEM-image for screen-printed and light-induced plated silver. (b) SEM-image for glass frit layer after bulk silver was eliminated.

ing high series resistance and its results are similar to those outlined in Tables 1 and 2.

The difference LIP and electroplating is that electroplating requires the application of a voltage between the Ag anode and the front surface grids of the cell, while LIP does not need to connect the front surface grids. The voltage used in electroplating is used to provide the power for the transportation of electrons, while in LIP the voltage is applied to protect the Al-BSF. The effectiveness of electroplating on the improvement of the fill factor means that no special mechanisms exist in LIP compared to electroplating.

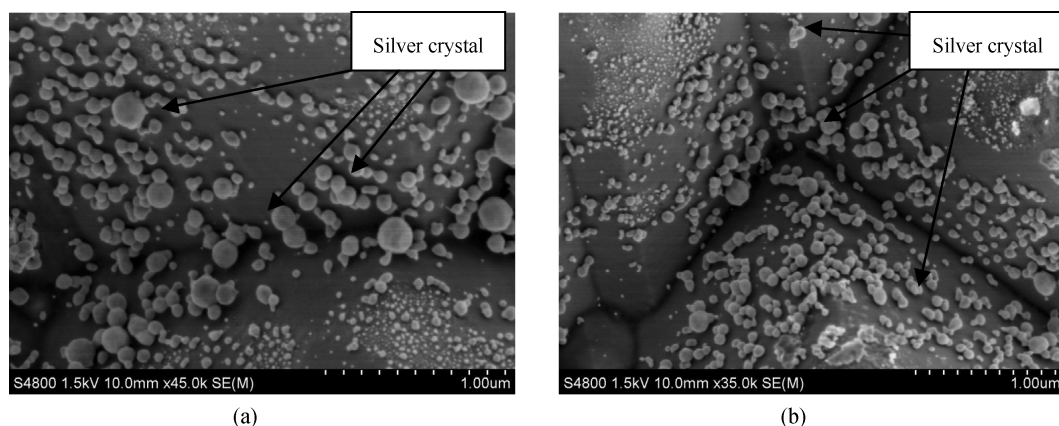


Fig. 5. (a) SEM-image after the glass frit layer is eliminated for a cell with a fill factor of 28%. (b) SEM-image after the glass frit layer is eliminated for a cell with a fill factor of 63%.

### 3.4. Micro-mechanisms involved in LIP

Porous screen-printed silver and compact plated silver are presented in Fig. 4(a). To investigate the mechanisms involved in LIP, the cells are rinsed in  $\text{HNO}_3$  for two hours. Bulk silver is eliminated in the process and SEM-images under the bulk silver are taken. Figure 4(b) shows the SEM-image for the glass frit layer after bulk silver is eliminated.

In a conventional contact formation model for screen-printed solar cell contacts, silver crystals embed in the emitter and are coated by a thin glass frit layer after the cooling down phase, with the bulk silver lying on the top. As shown in Fig. 4(b), holes are formed in the glass frit layer. Electrolytes will penetrate into the holes during LIP and thus plate silver contacts with the silver crystals below the glass frit layer.

For further investigations into the micro-mechanisms of the improvement of fill factors by LIP, two cells C and D are selected, with their fill factors at 28% and 63%, respectively. The fill factor of cell C ascends to 61% after LIP. The two cells are rinsed in  $\text{HNO}_3$  for 2 h and in 40 wt% HF for several minutes sequentially. After the glass frit layer is eliminated, the silver crystals are exposed. Silver crystal density is investigated by SEM.

In Figs. 5(a) and 5(b), almost the same silver crystal density is observed, which resulted in a low series resistance for cell C after LIP. A high density of silver crystals means a high potential for reducing a cell's series resistance.

## 4. Conclusion

The poor fill factor caused by high series resistance for a solar cell may be improved by using the LIP process. After the LIP process, the series resistance is significantly reduced, which results in the rise of the fill factor of solar cells. Electrolytes penetrate into the holes in the glass frit layer and the plated silver contact with idle silver crystals. A high silver crystal density is also observed for cells with low fill factors, which validates the fact that the improvement for cells with a poor factor after LIP should benefit from sufficient exploitation of the high density silver crystals formed during the firing process. Though solar cells with high fill factors benefit little from LIP, LIP is helpful in reducing the increasing contact resistance

when narrowing the grids. Also LIP provides a new method for the optimization of the cells which are limited by their “bad” metallization contact performances, such as for nanowire cells and radial junction solar cells. The “bad” contact performance encountered with nanowire cells and radial junction cells may benefit from LIP.

## References

- [1] Liu Wen, Li Yueqiang, Chen Jianjun, et al. Optimization of grid design for solar cells. *Journal of Semiconductors*, 2010, 31(1): 014006
- [2] Lee J H, Lee Y H, Ahn J Y, et al. Analysis of series resistance of crystalline silicon solar cell with two-layer front metallization based on light-induced plating. *Sol Energy Mat Sol C*, 2011, 95(1): 22
- [3] Pysch D, Mette A, Filipovic A, et al. Comprehensive analysis of advanced solar cell contacts consisting of printed fine-line seed layers thickened by silver plating. *Progress in Photovoltaics: Research and Applications*, 2009, 17(2): 101
- [4] Huljic D M, Ballif C, Hessler-Wyser A, et al. Microstructural analyses of Ag thick-film contacts on n-type silicon emitters. *3rd World Conference on Photovoltaic Energy Conversion*, 2003, 1: 83
- [5] Mette A, Schetter C, Wissen D, et al. Increasing the efficiency of screen-printed silicon solar cells by light-induced silver plating. *4th World Conference on Photovoltaic Energy Conference*, 2006, 1: 1056
- [6] Neuhaus D H, Monzer A. Industrial silicon wafer solar cells. *Advances in Opto Electronics*, 2007: 1
- [7] Mette A, Richter P L, Horteis M, et al. Metal aerosol jet printing for solar cell metallization. *Progress in Photovoltaics: Research and Applications*, 2007, 15: 621
- [8] Gauthier M, Grau M, Nichiporuk O, et al. Industrial approaches of selective emitter on multicrystalline silicon solar cells. *24th European Photovoltaic Solar Energy Conference*, 2009: 1875
- [9] Hilali M M, Rohatgi A, Khadilkar C, et al. Understanding and development of Ag pastes for silicon solar cells with high sheet-resistance emitters. *19th European Photovoltaic Solar Energy Conference*, 2004: 1300
- [10] Kray D, Bay N, Cimiotti G, et al. Industrial LCP selective emitter solar cells with plated contacts. *Photovoltaic Specialists Conference*, 2010: 667
- [11] Ebong A, Rounsaville B, Cooper I B, et al. High efficiency silicon solar cells with ink jetted seed and plated grid on high sheet resistance emitter. *Photovoltaic Specialists Conference*, 2010: 1363